

# Suggestions for the Structure of Kernel Software in Intelligent Seismic Nets

George R. Daghish, *Member, IAENG*, Yuri P. Sizov, *Member, EAGS*

**Abstract**—This paper provides a description of a prototype scheme which suggests a Software Structure to be embedded within a Seismic Net in order to rapidly locate Epi- and Hypocentral coordinates of, in particular, Teleseismic Events that are likely to generate Tsunamis. As yet, not all proposed elements for this are in place. However, the current state of development is deemed sufficient to warrant a brief exposition. The current structure is seen as enabling: Computer-aided Energy-onset Time Determination, Automatic provision of Epicentral Coordinates, Hypocentre Determination; then subsequently: Modeling the genesis and progression of Tsunamis and, using “Intelligenced” software, observing Fore- and Aftershock sequences.

**Index Terms**—Seismics, Epicentre, Tsunami, Warning, Modeling.

## I. INTRODUCTION

THE motivation for this work is as follows: given the severity of recent Natural Disasters involving coupling between Earthquake Fault Slips and Tsunami generation, it has been borne in upon the authors that efforts should be directed, in general, to facilitate those systems, such as monitoring, predictive and warning systems [5], [6], [10], [12], that would serve to mitigate these dire scenarios.

The problem, baldly stated, is as follows: we seek to automate the process of solving an Inverse Problem, in this case the restitution of Event Epicentre coordinates from Energy-onset Timings, in a reliable and rapid manner.

The technique we have chosen to follow up is: the solution of the above Inverse Problem by the rapid and possible automatic determination of Epicentral Coordinates that uses a Software Architecture which is to trigger either or both of:

- Tsunami warning procedures,
- Hypocentral Scan.

Manuscript received March 14, 2011; revised March 19, 2011.

G. R. Daghish is a Consultant with Independent Analysis and Computation at 9 Partridge Close, Frimley CAMBERLEY, Surrey. GU16 8PD. UK. +44 (0)1276 26942.

[George.daghish@tiscali.co.uk](mailto:George.daghish@tiscali.co.uk).

Yu. P. Sizov is with the GeoElectroMagnetic Research Institute, (where he is Scientific Secretary) at GEMRI. PO BOX 30. 142190 Troitsk, Moscow Region. RUSSIA. [Sizovyur1@yandex.ru](mailto:Sizovyur1@yandex.ru)

## II. SOFTWARE STRUCTURE

The root phase is the acceptance of incoming Seismograms at each participating “Out Station” with the concomitant digitization and deconvolution of each Seismogram from the receiving Seismometers’ collective impulse responses [1], [4]. Subsequently, a Fourier Transform process, featuring the Fast Fourier Transform (FFT), dubbed here as “Frequency Band Splitting”, (to be described below in Section III), takes place on each Seismogram.

Given that the most appropriate “Frequency Band” within each Seismogram Energy Structure has been selected, then Computer-aided Picks of Energy-onset timings are made using an interactive and backward-looping structure until the most faithful representation of the Energy-onset Timings is achieved (vide Section IV).

Data Objects are then transmitted to a “Centralised Facility” under the following headings:

- The Raw Seismogram,
- A selected wave-form within the user-defined frequency band,
- The selected waveform with Energy-onset markers as inserts.

Although the Central Facility would be equipped to resume the preprocessing that has occurred at any Out Station, the next phase is to select one of four given methods to present Energy-onset Timings as data for a combinatorial scan for the purpose of determining a set of most likely Epicentre candidates to be submitted to a final selection routine. This “final” calculation and selection of an Epicentre triggers the Hypocentral calculations. Such calculations are to take place in parallel with the determination process that decides whether or not the Epicentre corresponds to an “oceanic” location, potentially generating a Tsunami [10], [16].

As may be inferred from these remarks the process for finding the Epicentral coordinates is backward-looping to the point of the Energy-onset Timing presentation to the combinatorial scan.

## III. FOURIER PROCESSING USING THE FFT AS A BAND-PASS FILTER

Using the Fourier Coefficients initially generated for the incoming Accelerogram, namely  $z_i = P_i + jQ_i$ , we can add a Band Pass selection of frequencies to input to the FFT

integration processes. This enables us to clearly see how the contribution of specific frequency bands forming the wave structures, emanating from the Seismic Event in question, is made [4], [18].

This process could be referred to as frequency-band splitting where discrete bands are chosen with specific widths for each band.

However, a more ideal procedure would be represented at this juncture if the width of each instantaneous band was selected dynamically while the basal frequency of the "Band Window" was made to slide through some subset of the frequencies present in the incoming Accelerogram. For each such "Band Window" and its basal frequency the required integration should take place. Such a procedure would allow a complete review of those resultant waveforms most apt to demonstrate the arrivals of the set of P-; S-; L- and R-waves species for the ultimate purposes of their Event Location.

#### IV. GENERATION OF ENERGY-ONSET TIME MARKERS

This can be attempted in at least two different ways:

1. Using the FFT on the Seismogram to determine the Power Spectra for the two time-segments that together make up the detection scheme.
2. Integrating the absolute values of the Seismogram sample data to obtain an indication of the mean power values for the two time-segments forming the detection mechanism.

The first method was found to be slow. The Trapezoidal Integration in the second method proves to be more rapid. The essence of both methods is given by the following general consideration:

There are many suggestions to be taken from successful monitoring systems for this aspect [2], [3], [13]. One basic observation is as follows:

Given an onset of any of the wave types, (in particular the potential arrival of P-energy), then we might say, following [2]:

$$\alpha_p(\tau_\alpha) = \frac{1}{\tau_\alpha} \int_{t-\tau_\alpha}^t |A(t)| dt$$

$$\beta_p(\tau_\beta) = \frac{1}{\tau_\beta} \int_{t-\tau_\beta}^t |B(t)| dt$$

$$\gamma = \frac{\alpha_p}{\beta_p},$$

This is onset detection by energy considerations, and the following definitions apply:

$A(t)$  displacements by incident energy,

$\tau_\alpha$  time period for this integration,

$B(t)$  also displacements by incident energy,  
 $\tau_\alpha$  time period for this latter integration.

We must have that  $A(t) \supset B(t)$  and that  $\tau_\alpha \ll \tau_\beta$ .

If, then, the ratio " $\gamma$ " exceeds a prescribed threshold ( $\geq Unity$ ) an onset is deemed to have occurred.

In both cases, when the ratio,  $\gamma$ , is exceeded, then a marker is placed against the lead sample belonging to the short time-segment. These results are held in file form and can be further refined.

#### V. A DIRECT AND AN INDIRECT MEANS OF DETERMINING AN EPICENTRE

For the Indirect means, we can say: for two separate arrivals at a given point in space, originating from the same source and having traveled with different velocities, we can write:

$$v_0 t = v_1 (t + \Delta t)$$

since each has passed over the same distance. Here  $v_0 t$  corresponds to the distance covered by that arrival with the greater velocity.  $v_1 (t + \Delta t)$  is the distance covered by the arrival with the lesser velocity and these two distances are the same.

The Time-to-Origin for the first arrival would be:

$$t = \frac{v_1}{v_0 - v_1} \cdot \Delta t$$

Thus, knowing  $\Delta t$ , the Time-difference between the two arrivals, by observations on the given Seismogram, we may write:

$$s = v_0 t = \frac{v_0 v_1}{v_0 - v_1} \cdot \Delta t$$

or

$$s = v_1 (t + \Delta t) = \left( \frac{v_1}{v_0 - v_1} + Unity \right) \cdot v_1 \Delta t$$

$s$  is the distance traveled from the source event by both wave-species. From this we can construct the diagram seen in **Figure 1**.

A and B are positions of the source and a receiving station, respectively.  $R_e$  is an effective Earth radius. In this sagittal diagram we find:

$$\alpha R_e = s \Rightarrow \alpha = \frac{s}{R_e}$$

$$r = R_e \sin \alpha; \quad R_0 = R_e \cos \alpha$$

In 3-space, the coordinates of the point O, in the same frame as the coordinates of point B, are:

$$a_0 = \frac{R_0}{R_e} \cdot a; \quad b_0 = \frac{R_0}{R_e} \cdot b; \quad c_0 = \frac{R_0}{R_e} \cdot c,$$

where the position of O is  $(a_0, b_0, c_0)$  and the position of B, (the station), is  $(a, b, c)$ . The point O therefore is the centre of a sphere:

$$(x - a_0)^2 + (y - b_0)^2 + (z - c_0)^2 = r^2$$

whose surface will include the source position at A. Thus for many stations and correspondingly observable  $\Delta t_i$  we get a set:

$$\{\alpha_i\} = \left\{ \frac{s_i}{R_e} \right\}$$

from which we might generate a system consisting of  $n$  spheres:

$$(x - a_i)^2 + (y - b_i)^2 + (z - c_i)^2 = r_i^2; \\ i = 0, (n-1)$$

whose mutual intersection (in the absence of error) can be thought to represent the position of Epicentral Coordinates for the source at A. This intersection is calculated as a linearised Least-Squares problem.

To the algorithm depicted in this has also been added a direct minimization of the Least-Squares cost function:

$$S_n = \sum_{i=0}^{i=n-1} \left( \sqrt{u_i} - r_i \right)^2; \\ u_i = (x - a_i)^2 + (y - b_i)^2 + (z - c_i)^2$$

which uses the output from the linearised version of the spherical equations as a starting point for its iterations. This is a Gauss/Newton iterative algorithm which will, firstly, use Jacobean matrices, but which will pull in a Hessian matrix if the main iteration sequence is going astray.

When both these methods have provided their respective solution vectors, in terms of two estimates of the Epicentral coordinates, the user is free to choose which estimate to accept as a basis for further processing.

For the Direct Estimation we give the following: the development for the simple Spherical Shell or lamina can be stated as a "conceptual" equation system – in particular:

$$\underline{x} \cdot \underline{a}_i = R^2 \cos \left( \frac{\bar{c}_0 (t_i - \Delta t)}{R} \right); \\ i = 0, (n-1)$$

where:

$\underline{x}$  is the Event Location,

$\underline{a}_i$  is the  $i^{th}$  sensor Location,

$R$  is a spherical shell radius,

$t_i$  is the  $i^{th}$  relative arrival time,

$\Delta t$  is the time-to-origin,

$\bar{c}_0$  is a wave propagation velocity.

All locations referred to here are in Cartesian coordinates. Then the solution vector for the above is:

$$\underline{s} = \begin{bmatrix} \underline{x} \\ \Delta t \\ \bar{c}_0 \end{bmatrix}$$

The Cartesians used here are coordinates within a Space Frame whose Origin coincides with the centre of the object Sphere. Thus in the foregoing:

$$\|\underline{x}\| \approx R; \quad \|\underline{a}_i\| \approx R.$$

This fact (or supposition) allows the following derivation:

An arc length is given by an expression such as:

$$R\theta$$

where  $R$  is the radius of the sphere or circle in question. Therefore considering the sphere on whose surface emissions are being transmitted, and removing the coordinate system origin to the centre of this sphere we get:

$$R \cos^{-1} \left( \frac{xa_i + yb_i + zc_i}{\|x\| \cdot \|a_i\|} \right) = \bar{c}_0 (t_i - \Delta t);$$

but:

$$\|x\| \cdot \|a_i\| = R^2$$

so:

$$R \cos^{-1} \left( \frac{xa_i + yb_i + zc_i}{R^2} \right) = \bar{c}_0 (t_i - \Delta t).$$

Transposing functions gives:

$$xa_i + yb_i + zc_i = R^2 \cos \left( \frac{\bar{c}_0 (t_i - \Delta t)}{R} \right);$$

$$t \in [0, (n-1)],$$

The solution of this system proceeds in two stages. An initial approximation to the solution vector is found by a scanning method using a “spider” moving over a region of a surface defined as a time/velocity space. Using this initial value, a Gauss/Newton “descent” method is employed to find the root of the system, considered as a non-linear Least-Squares cost function.

## VI. FEATURES OF THE HYPOCENTRAL CALCULATION

The Onset timings emanating from an actual or simulated event are made up, as follows, from a set  $T$  :

$$T \equiv \{t_j\}; \quad j = 0, (n-1)$$

Here the  $t_j$  are elements of a universal time running on a continuous time base, and represent arrivals of whatever wave species at Stations ( $j = 1$ ). Thus:

$$\bar{t} = \frac{1}{n} \sum t_j$$

We generate a spread of deviations about this mean as:

$$\tau_j = \{t_j - \bar{t}\}; \quad j=0, (n-1)$$

Similarly, using Point to Point Spherical Ray Tracing routines [3], [7], [8], [17], from any position on the upward scanning trajectory, we can find a set of deviations  $i$  for  $\{v_j\}_i; j = 0, (n-1)$ . In this,  $i$  indexes a point in the scan and  $j$  the set of active Seismic Stations. For each position in the scan we get:

$$RMS_i = \sqrt{\frac{1}{n} \sum_j (\tau_j - v_{j,i})^2}$$

It is this set of  $RMS$  values that is graphed against depth in **Figure 2**, and the infimum is taken to correspond to a Hypocentral Depth, in this case 20.08 kilometers.

In each set of deviations, corresponding to points on the scanning trajectory, and for each calculated Ray Arrival at each Station there is calculated a set of Radial Discrepancies:

$$P_i \equiv \{\rho_j\}_i; \quad j = 0, (n-1)$$

Indices are as before, and the Discrepancies are given by:

$$\rho_j = \frac{R_j - R_e}{R_e}$$

$R_j$  is the achieved Radius, at the required angular sweep to the given Station, by the Ray Trace algorithm, while  $R_e$  is a notional Earth radius, applicable to the particular case. This Discrepancy may be supplied as a percentage, as is done in **Figures 3** and **4**.

These two **Figures** display the maximum and minimum Discrepancies found for the set of rays to the set of active Stations for each point on the ascending trajectory, in this instance.

## VII. SUMMARY AND CONCLUSIONS

As stated at the outset the entire dynamic of this prototyping exercise is to show possibilities for the construction of a system that will:

1. Detect “oceanic” Epicentral Coordinates.
2. Make suppositions concerning the genesis of possible Tsunamis [3], [9], [10], [16].
3. Run predictive models of Tsunamis considered imminent [14], [15] (although the various possibilities for modeling these have not been treated in the present paper).
4. Make available and/or communicate information about such findings (e.g. expected Tsunami first arrival times), to appropriately placed warning systems, in good time.

5. Use “Intelligenced” software to observe Event Precursor Patterns [10], [11], [12] with an eventual view to indicating the likelihood of the occurrence of a future Event.

Further, in all of this, we note in passing, that the use of highly parallelised computational facilities is key to the rapid throughput of these suggested processes.

The way in which the various components of this relatively abstract scheme, as described in the present paper, are deployed in terms of a real Topographic Distribution, would be the subject of a further investigation..

In brief: outlying Stations would process individual Seismograms to the level of the insertion of Onset timing Markers and then transmit to a central facility whose front-end should find Epicentral Coordinates up to the level of the combinatorial scan and final selection.

This information is then passed, together with the collected P-wave and S-wave first onsets, to a highly parallelized facility which would perform  $n$  individual Ray Traces in parallel, thus establishing more rapidly the Hypocentral Depth. Such routines would be run with a high degree of parallelism.

The same facility would then, if required, embark upon the proposed detailed Tsunami Modeling Phase and, during this, the front-end would process a coarser version of the Model for the spreading Tsunami, within the most likely zones of the stricken region.

#### REFERENCES

- [1] “Geophysical Signal Processing”. Robinson EA, Durrani TS, et al. Prentice-Hall. 1985.
- [2] “Principles and Applications of Microearthquake Networks”. Lee WHK, Stewart SW. Academic Press. 1981.
- [3] “Advances in Seismic Event Location”. Thurber CH, Rabinovitz N. Springer. 2000.
- [4] “Instrumentation in Earthquake Seismology”. Havskov J, Alguacil G. Springer. 2004.
- [5] “Global Dynamics of the Earth”. Saladin R, Vermeersen B. Springer. 2004.
- [6] “Global Tectonics”. Keary P. Wiley-Blackwell. 2009
- [7] “Seismology and the Structure of the Earth”. Dziewonsky A. Elsevier. 2009.
- [8] “The Dynamic Structure of the Deep Earth: an Interdisciplinary Approach”. Karato S-I. Princeton University Press. 2003.
- [9] “Numerical Modeling for Earthquake Source Imaging: Implications for Array Design in Determining the Rupture Process”. Yi-Ling Huang, Bor-Shouh Huang, Chengsung Wang, Kuo-Liang Wen. TAO, Vol. 15, No. 2, 133-150. 2004.
- [10] “The Complex Faulting Process of Earthquakes”. Koyama J. Springer. 1997.
- [11] “Reports on Ocean-going Drilling Platforms: ‘Ocean Monster Shows Hidden Depths’ ”. Black R. BBC News, Japan. May 2009.
- [12] “Seismic Hazard and Risk Analysis”. McGuire RK. EERI. 2004.
- [13] “Detection and Classification of Acoustic and Seismic Events using a Semi-Markov Energy Dynamical Model”. Pang Sze Kim, Geok Lian Oh, Shanguo Lu, Adrian Yap Cheng Lock. IMA Conference on Mathematics in Defence 2009. CD. IMA. 2009.
- [14] “Tsunami Phenomenon and Warning System”. Sizov Yu. P., Kopytenko Yu., A., Cherkashin Yu., N., Ismagilov V., S.

MARELEC-09 Conference. Stockholm. Sweden. CD. 7-9 July 2009.

- [15] “Numerical Modeling of the Global Tsunami”. Kowalik Z., Knight W., Logan T., Whitmore P. Science of Tsunami Hazards, Vol. 23, No 1, pp 40 et seq. 2005.
- [16] “Modeling the Asian Tsunami Evolution and Propagation with a new Generation Mechanism and a Non-Linear Dispersive wave Model”. Rivera P. C. Science of Tsunami Hazards, Vol. 25, No 1, pp 18 et seq. 2006.
- [17] “A Perturbation Method, which achieves accurate Point-to-Point Ray Traces, and its Context”. Daglish G. R. ICSPATA 2010, July. Jiao Tong University, ShangHai, PR China. 2010.
- [18] “Mathematics for Seismic Data, Processing and Interpretation”. Carmina A. R., Janacek G. J. Graham & Trotman. 1984.

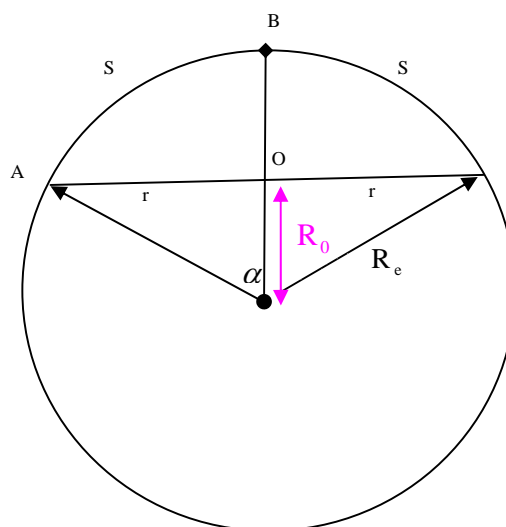


Figure 1. Diagrammatic Epicentre Geometry

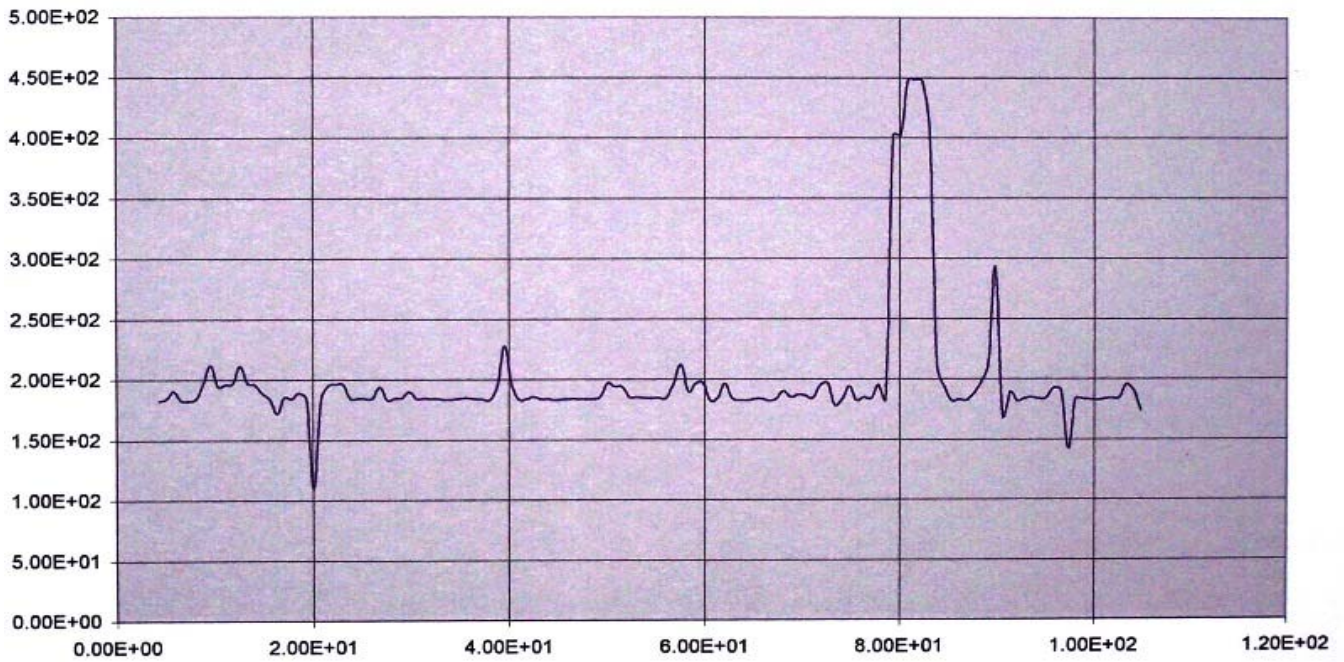


Figure 2. Tracking rms Residuals to Establish Hypocentre. Epicentre at [31.25 S, 80.26 W]. Radial Discrepancy was  $4.707e-05$ . Hypocentre at 20.08 kilometers.

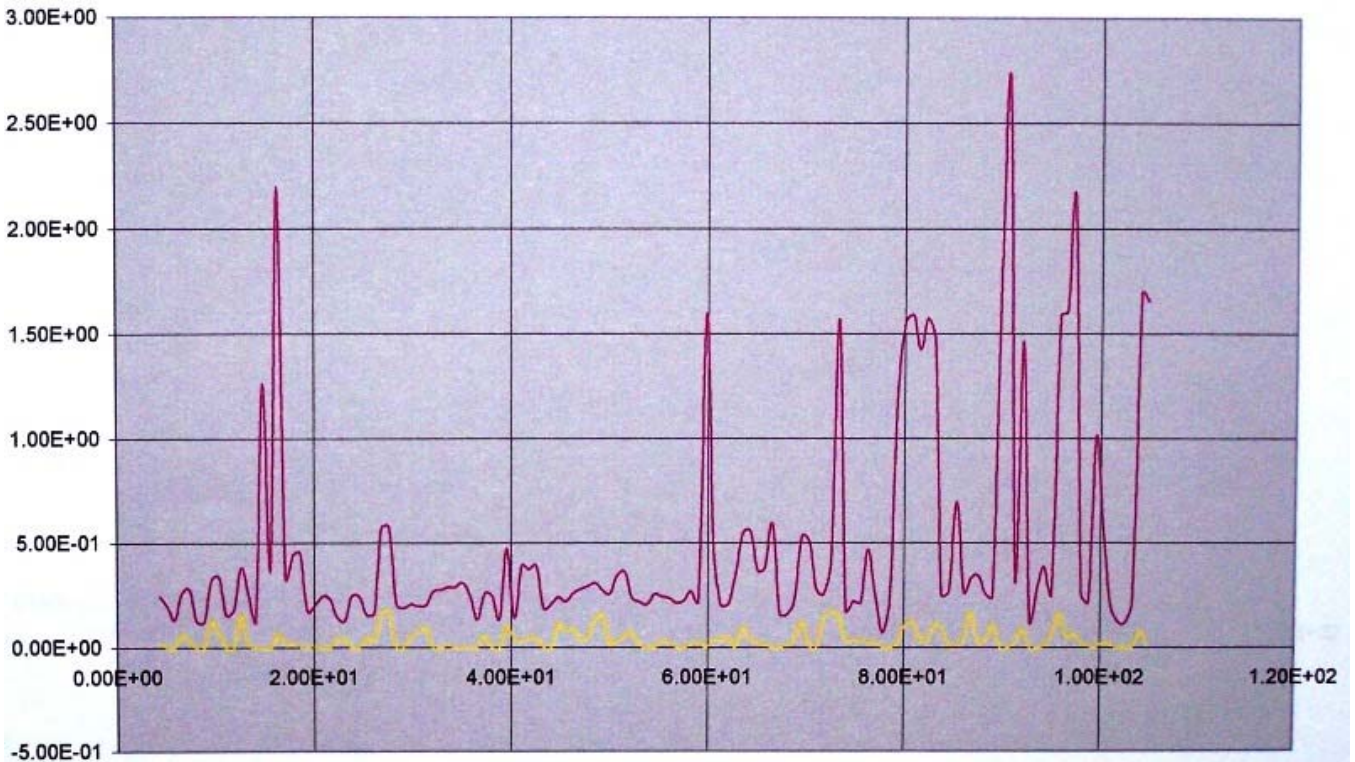
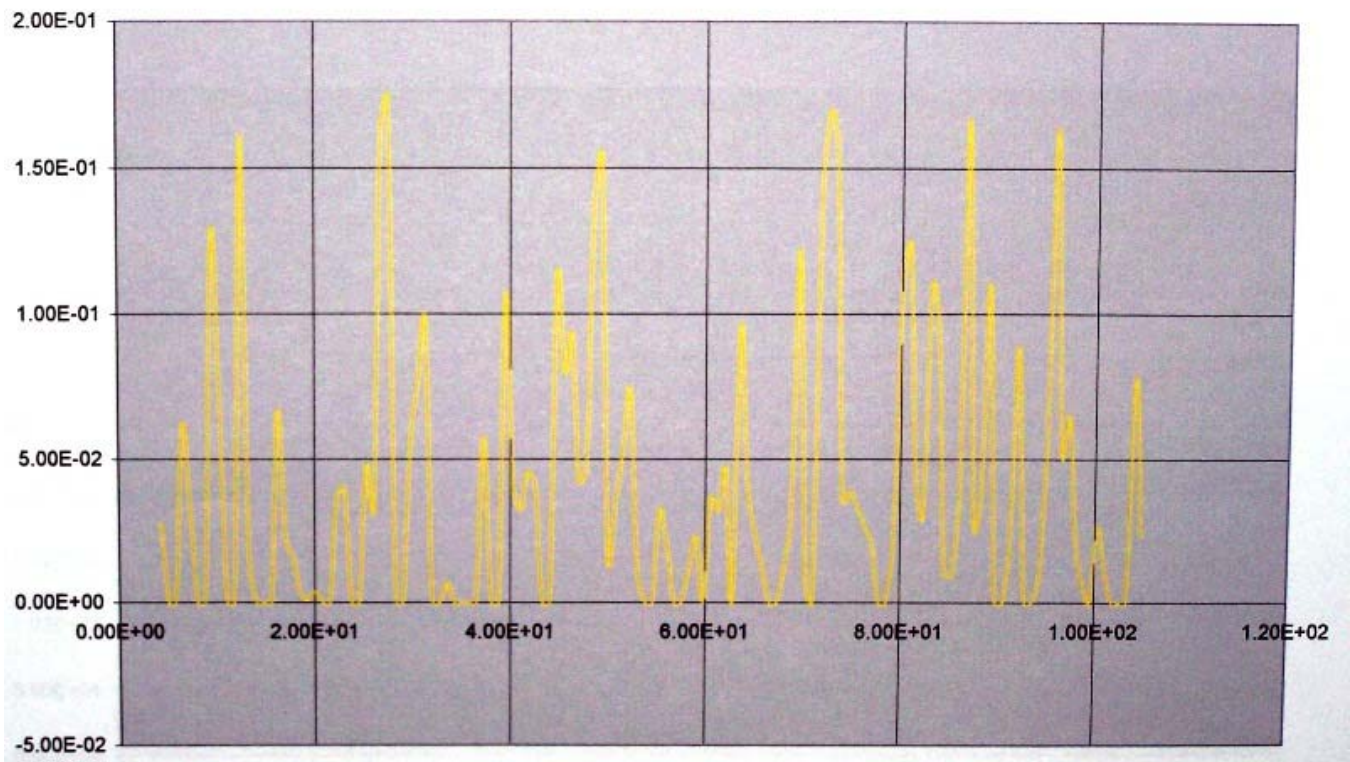


Figure 3. Tracking Radial Discrepancy (Red – Maximum; Yellow – Minimum) for Ray Paths realized at the set of Stations.



**Figure 4. Tracking Minimum Radial Discrepancy for ray Paths realized at the set of Stations.**